IEEE Access
Multidisciplinary | Rapid Review | Open Access Journal

IEEE POWER & ENERGY SOCIETY SECTION

Received March 30, 2021, accepted April 10, 2021, date of publication April 13, 2021, date of current version April 20, 2021.

Digital Object Identifier 10.1109/ACCESS.2021.3072841

Harmonic Vector Error Analysis Based on Lagrange Interpolation

ZHAOYUN ZHANG[1], (Senior Member, IEEE), QITONG WANG[1,2], AND ZHI ZHANG[1]

[1]College of Electronic Engineering and Intelligence, Dongguan University of Technology, Dongguan 523808, China
[2]School of Automation, Guangdong University of Technology, Guangzhou 510006, China

Corresponding author: Zhaoyun Zhang (18927491998@163.com)

This work was supported in part by the Guangdong Science and Technology Foundation of China under Grant 2017A010104023.

ABSTRACT With the development of smart substations and the promotion of 61850 standards, sampling values based on IEC61850-9-2 have become an important part of smart substation construction. With the popularization and application of the sample value (SV), the interpolation algorithm has been increasingly used in protection, measurement, control, wave recorder and power quality applications. However, the error in the interpolation algorithm poses a challenge to its use. This paper describes the basic methods of linear Lagrange and parabolic Lagrange interpolation and presents maximum theoretical values for the interpolation error when Lagrange linear and second-order approximations of sinusoidal signals are performed. The single-point error of each sampling point is analyzed using the remainder equation, and the harmonic error of the Fourier transform after interpolation is strictly mathematically derived. Finally, the accuracy of the theory is verified by real measurement data, and suggestions for the application of the interpolation method are introduced.

INDEX TERMS Intelligent substation, Lagrange interpolation, error analysis, harmonic.

I. INTRODUCTION

Harmonic measurement and vector calculation are important tasks in substations, utilities and users [1]. In the early substations, there was a situation of asynchronous sampling, and it was necessary to calculate all channels to the same time value through a certain method. Among them, Lagrange interpolation is the most widely used method. With the construction of smart substations, it has been more than ten years since the construction of smart substations, and there is currently a consensus on sampling values, i.e., the use of IEC 61850-9-2 [2]. Reference [3] presented a 10-bit 600 MS/s 4-channel time-interleaved successive approximation register analog-to-digital converter (ADC). A background calibration algorithm using Lagrange polynomial interpolation was introduced to calibrate the timing skew. In digital substations, it is necessary to correct the time sequence of the measuring device, so the application of Lagrange in the intelligent substation is of great significance.

At present, the measurement of electrical quantity in smart substations is mostly point-to-point synchronous sampling, but the point-to-point sampling method has no time scale. It is necessary to interpolate the collected electrical quantity before the time synchronous electrical quantity can be measured. The current commonly used interpolation methods include linear Lagrange interpolation (first-order Lagrange interpolation), parabolic Lagrange interpolation (second-order Lagrange interpolation), Newton interpolation, and Hermite interpolation [4]–[6]. The advantage of the Lagrange interpolation method is that it does not require solving linear equations, it can effectively reduce the rounding error for a large amount of data, and the calculation effect is much better than that of power series interpolation [7]. The Lagrange error must be minimized. This algorithm is used in the interval, and the interpolation accuracy increases within a certain range by increasing the number of interpolation points [8]. Reference [9] introduced an effective digital calibration algorithm based on Lagrange interpolation for the phase shift factor of electronic meters, which reduces the phase shift of static meters. Reference [10] presents a filter design technique based on quasi multiple resonators that approximates the exact multiple resonators technique. The design is simpler thanks to usage of the Lagrange interpolation technique. Reference [11] introduced a new method to construct linear-phase Lagrange interpolators using an odd number of base points. In [12], a fractional delay filter

The associate editor coordinating the review of this manuscript and approving it for publication was Arpan Kumar Pradhan.

design method based on the impulse response of the truncated Lagrange interpolation filter was proposed. Reference [13] proposed a new Lagrange interpolation filter structure with linear complexity. The design of this structure is not only efficient but also has dynamic update characteristics.

Fundamental and harmonic analysis and calculation are the basic functions of recorders, measurement devices, power quality analysis devices, etc. [14]–[16]. The most commonly used analytical method is fast Fourier transform (FFT) analysis. Most of the harmonic calculations are based on the FFT algorithm. For example, in reference [17], because of the limitation of the FFT due to the fence effect and spectral leakage, the accuracy of the harmonic analysis is low; therefore, a characteristic harmonic analysis algorithm based on spectral refinement and interpolation was proposed. Reference [18] proposed a new method for the harmonic analysis of industrial power systems based on a windowed FFT with high accuracy, fast calculation speed and easy implementation. These algorithms are implemented based on FFT, and the FFT algorithm forms the basis for the analysis of the fundamental wave and harmonics of the power grid.

After we interpolate the original waveform and implement the FFT algorithm, the resulting amplitude produces an increased error, as identified in previous studies. Reference [19] also proposed a new algorithm of polynomial cosine window interpolation for the FFT error for harmonic analysis and amended the FFT results. In reference[13], it was noted that the FFT has a large error in asynchronous sampling, so it cannot obtain accurate harmonic parameters during motor testing. To reduce the effect of asynchronous sampling on FFT to improve the accuracy of harmonic analysis in motor testing, this paper improves the original algorithm by adding windows and interpolation. Reference [19] analyzed the error of a single sampling point during linear Lagrange interpolation. However, in the current article, we do not perform impact analysis of various interpolation algorithms on the results of the FFT algorithm (maximum error estimation).

Most of the previous studies have analyzed only the point-to-point error after interpolation and combined the Lagrange interpolation method with power electronics to measure the wave and analyze the error [20]. In reference [21], to resolve the spectral leakage caused by asynchronous sampling, a Hilbert reactive power calculation method based on data preprocessing was proposed. In this paper, only the point-to-point error was studied, and the theoretical error analysis after the FFT as not included. Only by simulating the image method can we obtain an approximate error range. At present, there is no literature on the maximum theoretical value of the interpolation error for the Lagrange linear and second-order approximation of sinusoidal signals. Therefore, this paper aims to analyze the effect of the first- and second-order Lagrange interpolation algorithms on the results of the FFT algorithm, present maximum theoretical values for the interpolation error when Lagrange linear and second-order approximations of sinusoidal signals are performed, estimate the maximum error, provide a theoretical basis for the monitoring and measurement of intelligent substations, and verify the accuracy of the analysis with a practical case.

II. BASIC ALGORITHM OF HARMONIC ANALYSIS

This paper needs to analyze the various harmonics in the signal separately, the basis of the analysis in this paper is the basic algorithm of harmonic analysis. For convenience of analysis, the original input signal is assumed to be

$$x(t) = A\sin(2\pi fmt) \tag{1}$$

where f is the fundamental frequency (50 or 60 Hz for most power grids). This paper selects 50 Hz for analysis; A is the signal amplitude, which is 1 in this paper. Depending on the nature of the signal, its unit is changeable, so its unit is not discussed in this paper; and m is the harmonic number. The fundamental wave corresponds to m = 1, and t is the time.

The process of obtaining the final harmonic amplitude according to the sampling value includes the following steps:

A. SAMPLING

In the power system measurement device, power analysis device, and recorder, the original signal is first regularly sampled, and N points are sampled at equal intervals in a fundamental period to obtain the original sampling points; the interval is written as N-point sampling. The data after sampling at equal intervals are recorded as:

$$x_0, x_1 \ldots x_{n-1}$$

For the convenience of analysis, 80-point sampling is used in the example, i.e., the sampling period is 250 us. The analysis methods described later are also applicable to other sampling rates.

B. INTERPOLATION

At present, the communication protocol used in smart substations is mainly based on IEC61850-9-2. The point-to-point mode without time stamp requires the receiver to synchronize according to the received time and data, so interpolation is needed for synchronization.

Interpolation is used mainly to restore all channels to the values of the same time for the sampled sequence. Generally, interpolation is only interpolated and not extrapolated. For example, channel 1 receives data at 0 μs, 250 μs, 500 μs…over a second; channel 2 receives data at 100 μs, 350 μs, 600 μ…over a second; and channel 3 receives data at 200 μs, 450 μs, 700 μs…over another second. In some applications, the values must be restored to the same time. For example, if channel 1 is used as the reference, channel 2 must be traced back to 100 μs, and channel 3 must be traced back to 200 μs. In this case, interpolation is required.

There are many methods of interpolation. At present, linear Lagrange interpolation and parabolic Lagrange interpolation are often used. Corresponding to the 500 μs moment of channel 1, if linear Lagrange interpolation is used, channel 2 must use the 350 μs and 600 μs data for interpolation, and

channel 3 must use the 450 μs and 700 μs data for interpolation; if parabolic Lagrange interpolation is used, channel 2 must use 100 μs, 350 μs and 600 μs data for interpolation. Channel 3 must use 200 μs, 450 μs and 700 μs data for interpolation. This article describes specific methods in the third and fourth parts of this process; finally, we simultaneously calculate the values of all channels.

C. FAST FOURIER TRANSFORM (FFT)

The final step of harmonic analysis is to obtain the amplitude of the harmonics from the sampling points. Generally, the FFT is used to calculate the real and imaginary parts of the sinusoidal signal.

Here, the simultaneous engraved points in step B are subjected to the Fourier algorithm, and the amplitude is obtained according to [22]. The real part is:

$$a_1 = \frac{1}{N}\left[2\sum_{k=1}^{N-1} x_k \sin\left[k\frac{2\pi}{N}\right]\right] \tag{2}$$

where N is the number of sampling points.

The imaginary part is:

$$b_1 = \frac{1}{N}\left[x_0 + 2\sum_{k=1}^{N-1} x_k \cos\left(k\frac{2\pi}{N}\right) + x_N\right] \tag{3}$$

D. AMPLITUDE CALCULATION

$$\dot{X}_1 = \frac{1}{\sqrt{2}}(a_1 + jb_1) \tag{4}$$

In the existing literature, analysis of the error caused by interpolation generally analyzes only the error of step 2 (i.e., the single-point error caused by interpolation) and not the error of step 3 (i.e., the final harmonic error). However, for most electric power workers, the final harmonic error is of interest. This article provides a practical method to solve this problem: linear Lagrange interpolation.

III. LINEAR LAGRANGE INTERPOLATION

A. INTERPOLATION METHOD

Linear Lagrange interpolation, which is also known as first-order Lagrange interpolation, is currently the most widely used interpolation algorithm.

According to the sampling principle, the device regularly samples and sequentially obtains two sampling points (x_{k-1}, y_{k-1}), (x_k, y_k), where x is the sampling time and y is the sampling value at that moment. According to the Lagrange interpolation principle, an approximate function $L_1(x)$ is constructed, so $L_1(x)$ passes through points (x_{k-1}, y_{k-1}) and (x_k, y_k); then:

$$L_1(x) = y_k\frac{x - x_{k-1}}{x_k - x_{k-1}} + y_{k-1}\frac{x - x_k}{x_{k-1} - x_k} \tag{5}$$

According to the principle that the interpolation algorithm only interpolates, the sample value corresponding to $x_{k-1} \le x \le x_k$ can be calculated using this equation. For example, as mentioned, corresponding to the 500 μs moment of channel 1, channel 2 uses 350 μs and 600 μs data to interpolate according to the above formula, and channel 3 uses 450 μs and 700 μs data to interpolate according to equation (5).

B. SINGLE-POINT ERROR

The sampling point obtained by interpolation function $L_1(x)$ is a kind of "observed value" relative to the value given by the original signal curve, and there is a certain error from the "true value" on the original signal curve. This part studies the maximum error between the "true value" and "observed value" of a single point. According to Lagrange interpolation, from a to b the residuals are:

$$\begin{aligned} R_1(x) &= f(x) - L_1(x) \\ &= \frac{|f''(\xi)|}{2!}(x - x_k)(x - x_{k+1}) \quad \xi \in (a, b) \end{aligned} \tag{6}$$

The derivation of $R_1(x)$ shows that when $x = \frac{x_k + x_{k+1}}{2}$, the single-point error is the largest, and the maximum value is:

$$\begin{aligned} R_1\,\max &= A\frac{|\mathrm{m}^2\sin(\xi)|}{2!} \times \frac{1}{4} \times \left(\frac{2\pi}{N}\right)^2 \\ &= A4.93^*\frac{\mathrm{m}^2}{N^2}|\sin(\xi)| \end{aligned} \tag{7}$$

where N is the number of sampling points,

A is the amplitude of the signal,

m is the number of harmonics.

These parameters have the same meaning as here in the following sections.

Equation (7) shows that the maximum error varies with the interpolation time.

C. ERROR ANALYSIS AFTER FFT

Based on the single-point error, this article focuses on the error analysis of the harmonics after the FFT.

Equation (7) shows the range of the single-point error. The error range is different at different interpolation positions. From the equation, the maximum error function of each point and the original signal function are sinusoidal functions, so they can be directly superimposed on each other. At this time, there are two situations in the error analysis:

1) CASE 1

The value of the original signal curve is increased in the same direction by error value R_1 max, i.e., increased away from the coordinate axis based on the true value, as shown by the point of the observed value b-curve in Figure 1 (Figure 2 shows a partial magnified view of Figure 1); the error function at this time is:

$$R_1\,\max = A4.93\frac{\mathrm{m}^2}{N^2}\sin(\xi) \tag{8}$$

2) CASE 2

The value of the original signal is increased by an error value in the opposite direction of R_1 max, i.e., increased near the

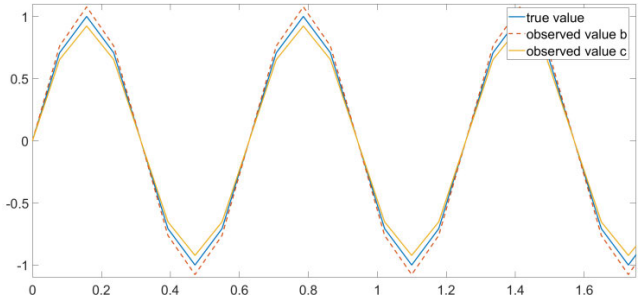

FIGURE 1. Harmonic figure error of m = 10 after FFT application.

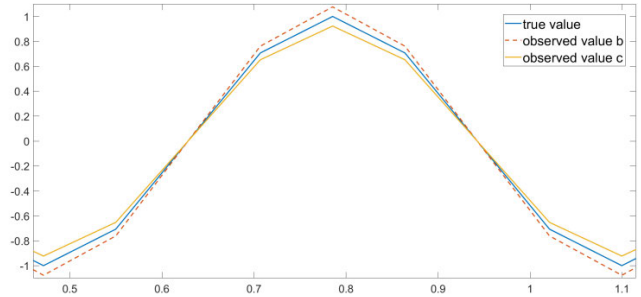

FIGURE 2. Figure error of m = 10 harmonic part waveform after FFT application.

TABLE 1. Theoretical calculation error of each harmonic when N = 80.

Harmonic number	Theoretical maximum positive error	Theoretical maximum negative error
1	0.0008	-0.0008
2	0.003	-0.003
13	0.13	-0.13
15	0.173	-0.173
20	0.308	-0.308
25	0.48	-0.48

coordinate axis based on the true value, as shown by the point of the observed value c-curve in Figure 1 (Figure 2 shows Figure 1 with local magnification). The error function at this time is:

$$R_1 \max = -A4.93 \times \frac{\mathrm{m}^2}{N^2} \sin(\xi) \tag{9}$$

These two cases are the maximum probability of error.

In these two cases, a vector with the same modulus $A4.93\left(\frac{m}{N}\right)^2$ in the same direction is superimposed on the previous points of the original signal, so the calculated errors are identical: $A4.93\left(\frac{m}{N}\right)^2$.

Therefore, according to the calculation, when the amplitude A of the original signal a is 1 and the sampling point N is 80, the errors of different harmonic orders are shown in Table 1.

If the sampling points N is 200 the errors of different harmonic orders is shown in Tables 2.

TABLE 2. Theoretical calculation error of each harmonic when N = 200.

Harmonic number	Theoretical maximum positive error	Theoretical maximum negative error
1	0.00012	-0.00012
2	0.0004	-0.0004
10	0.0123	-0.0123
20	0.0493	-0.0493
40	0.1972	-0.1972
60	0.4437	-0.4437

IV. PARABOLIC LAGRANGE INTERPOLATION

A. INTERPOLATION METHOD

The parabolic Lagrange interpolation method, which is also known as the second-order Lagrange interpolation method, is different from the linear interpolation method: 3 sampling points are selected by the parabolic interpolation method. This interpolation method is also widely used.

Similar to linear interpolation, according to the sampling principle, the equipment samples at fixed time to obtain three sampling points: (x_{k-2}, y_{k-2}), (x_{k-1}, y_{k-1}), (x_k, y_k), where x is the sampling time and y is the sampling value at that time. According to the construction characteristics of linear interpolation polynomials, a quadratic function $l_i(x)(i = k, k-1, k-2)$ is constructed for each sampling point x_i to satisfy:

$$l_i(x_i) = 1, \quad l_j(x_j) = 0, \ (i \neq j), i, j = k, k-1, k-2$$

where:

$$l_k = \frac{(x - x_{k-1})(x - x_{k-2})}{(x_k - x_{k-1})(x_k - x_{k-2})} \tag{10}$$

$$l_{k-1} = \frac{(x - x_k)(x - x_{k-2})}{(x_{k-1} - x_k)(x_{k-1} - x_{k-2})} \tag{11}$$

$$l_{k-2} = \frac{(x - x_k)(x - x_{k-1})}{(x_{k-2} - x_k)(x_{k-2} - x_{k-1})} \tag{12}$$

Equations (10), (11) and (12) are interpolation basis functions of the parabolic Lagrange interpolation. Finally, an approximate function is constructed according to the principle of Lagrange interpolation so that the crossing points of (x_{k-2}, y_{k-2}), (x_{k-1}, y_{k-1}), and (x_k, y_k) are as follows:

$$\begin{aligned} L_2(x) &= l_k(x)y_k + l_{k-1}(x)y_{k-1} + l_{k-2}(x)y_{k-2} \\ &= \underbrace{\frac{(x - x_{k-1})(x - x_{k-2})}{(x_k - x_{k-1})(x_k - x_{k-2})}}_{l_k(x)} y_k \\ &\quad + \underbrace{\frac{(x - x_k)(x - x_{k-2})}{(x_{k-1} - x_k)(x_{k-1} - x_{k-2})}}_{l_{k-1}(x)} y_{k-1} \\ &\quad + \underbrace{\frac{(x - x_k)(x - x_{k-1})}{(x_{k-2} - x_k)(x_{k-2} - x_{k-1})}}_{l_{k-2}(x)} y_{k-2} \end{aligned} \tag{13}$$

According to the principle of the interpolation algorithm with only interpolation, the corresponding sampling value can be calculated using equation $x_{k-1} \leq x \leq x_k$. For example, at 500 μs for channel 1, channel 2 uses the 100 μs, 350 μs and 600 μs data for interpolation according to the above formula, and channel 3 uses the 200 μs, 450 μs and 700 μs data to interpolate according to equation (13).

According to interpolation equation (13), 250 μs of data can also be calculated by using 100 μs, 350 μs and 600 μs in channel 2. However, the 250 μs data are obviously delayed in data alignment at this time, which is not recommended.

B. SINGLE-POINT ERROR

The value given by a point relative to the original signal curve is an ''observed value'', which has a certain error relative to the ''true value'' on the original signal curve. This part studies the maximum error between the ''true value'' and ''observed value'' of a single point.

Similar to linear interpolation, the sample value obtained by the parabolic Lagrange interpolation function is the ''observed value'', which has an error compared to the ''real value'' on the original signal curve, so the maximum error must be further analyzed. According to Lagrange interpolation, the remainder of the terms are as follows:

$$\begin{aligned} R_2(x) &= f(x) - L_2(x) \\ &= \frac{f'''(\xi)}{3!}(x-x_{k-2})(x-x_{k-1})(x-x_k) \quad \xi \in (x_{k-1}, x_k) \end{aligned} \tag{14}$$

Let the polynomial part of remainder equation (14) be:

$$g(x) = (x - x_{k-2})(x - x_{k-1})(x - x_k) \quad \xi \in (x_{k-1}, x_k)$$

The derivative of g(x) is obtained; when x is $\pm\frac{2\sqrt{3}\pi}{3N} + x_{k-1}$, g($x$) is maximal.

As mentioned, only the interpolation between x_k and x_{k-1} is considered; then, when $x = \frac{2\sqrt{3}\pi}{3N} + x_{k-1}$ has the maximum error, the maximum value of g(x) is

$$g(x)_{\max} = -0.3849\left(\frac{2\pi}{N}\right)^3 \tag{15}$$

The maximum error is obtained by substituting (14):

$$R_2(\max) = \text{A}0.512\,|\cos(\xi)|\,(\frac{m\pi}{N})^3, \quad \xi \in (x_{k-1}, x_k) \tag{16}$$

In the linear Lagrange interpolation, the interpolation error is maximal when the interpolation point is in the middle of x_k and x_{k-1}, i.e., when $x = \frac{\pi}{N} + x_{k-1}$ is adopted; if parabolic interpolation is used, the interpolation error can be expressed as follows:

$$R_2(x) = \text{A}0.512\,|\cos(\xi)|\,(\frac{m\pi}{N})^3 \tag{17}$$

Through the error equations (16) and (17), we observe the largest difference in error equation (7), which is obtained by linear Lagrange interpolation, and the sine function in the equation becomes a cosine function in the parabolic Lagrange interpolation. Similarly, the maximum error function obtained by parabolic Lagrange interpolation changes with time transformation.

C. ERROR ANALYSIS AFTER FFT

As in Section III, it is necessary to further study the final analysis error of each harmonic through the Fourier transform.

Similar to linear interpolation, the error range of different interpolation positions is shown in equations (16) and (17). Since the single-point error is an absolute value, we must discuss it according to different situations. Equation (17) shows that the error function is a cosine function, which is different from the error function in linear interpolation, which is a sine function. Therefore, because the true value = the observed value ± the error value, the discussion is divided into three situations. Take m = 10 as an example, i.e., the harmonic number is 10.

1) CASE 1

Based on the real value, an amount close to the coordinate axis is added; i.e., error $R_2^{(1)}$ max is added in the direction opposite to the original curve direction, and a maximum negative error is obtained. The point is described by the b-curve of the observed value in Figure 3 (Figure 4 shows a local magnified view of Figure 3).

In this case, the error function $R_2^{(1)}$ can be written as follows, and its function image is shown in Figure 5.

$$R_2^{(1)}(\text{t}) = \begin{cases} \text{-A}0.512\cos(m\omega\text{t})(\frac{m\pi}{N})^3 & 2\text{k}\pi \le m\omega\text{t} \\ & \le 2\text{k}\pi + \frac{\pi}{2} \\ \text{A}0.512\cos(m\omega\text{t})(\frac{m\pi}{N})^3 & 2\text{k}\pi + \frac{\pi}{2} \le m\omega\text{t} \\ & \le 2\text{k}\pi + \pi \\ \text{-A}0.512\cos(m\omega\text{t})(\frac{m\pi}{N})^3 & 2\text{k}\pi + \pi \le m\omega\text{t} \\ & \le 2\text{k}\pi + \frac{3\pi}{2} \\ \text{A}0.512\cos(m\omega\text{t})(\frac{m\pi}{N})^3 & 2\text{k}\pi + \frac{3\pi}{2} \le m\omega\text{t} \\ & \le 2\text{k}\pi + 2\pi \end{cases} \tag{18}$$

The continuous function is used to calculate the error. The real part and imaginary part of the error function $R_2^{(1)}$ and the original signal function are calculated. In addition, for the convenience of analysis, the constant part of $R_2^{(1)}$ is separated, and function $g_2^{(1)}(x)$ is obtained:

$$g_2^{(1)}(\text{t}) = \begin{cases} -\cos(m\omega\text{t}) & 2\text{k}\pi \le m\omega\text{t} \le 2\text{k}\pi + \frac{\pi}{2} \\ \cos(m\omega\text{t}) & 2\text{k}\pi + \frac{\pi}{2} \le m\omega\text{t} \le 2\text{k}\pi + \pi \\ -\cos(m\omega\text{t}) & 2\text{k}\pi + \pi \le m\omega\text{t} \le 2\text{k}\pi + \frac{3\pi}{2} \\ \cos(m\omega\text{t}) & 2\text{k}\pi + \frac{3\pi}{2} \le m\omega\text{t} \le 2\text{k}\pi + 2\pi \end{cases} \tag{19}$$

We have:

$$R_2^{(1)}(\text{t}) = A0.512 g_2^{(1)}(\text{t})(\frac{m\pi}{N})^3 \tag{20}$$

Here, $g_2^{(1)}(x)$ is a piecewise function. The number of segments is related to the number of harmonics. The error function

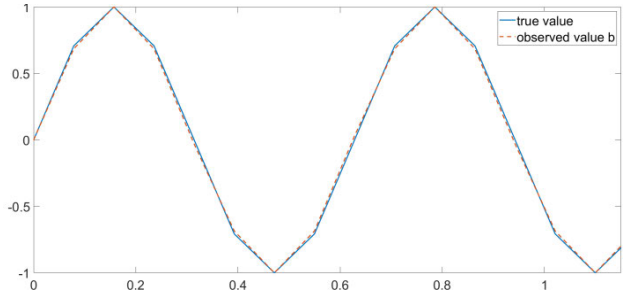

FIGURE 3. Harmonic figure error of case 1 with m = 10.

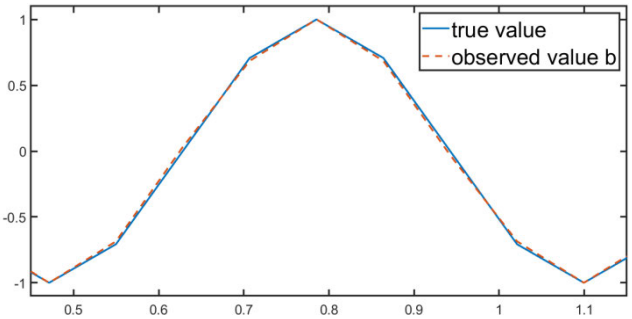

FIGURE 4. Figure error of m = 10 harmonic partial cycle amplification in case 1.

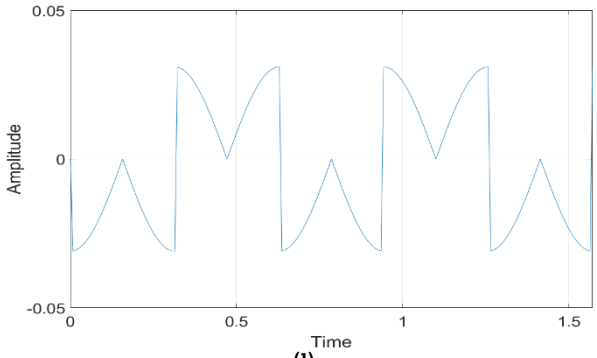

FIGURE 5. Curve of error function $R_2^{(1)}$ at m = 10.

of the m-th harmonic is divided into 4 m segments. The real part and imaginary part of $g_2^{(1)}(x)$ are obtained by an integral transformation of the real part and imaginary part of the Fourier transform. Without loss of generality, when m = 1, i.e., the fundamental wave is selected, the error function integral transformation is performed; the other harmonics only must increase the number of integral segments. The real part and imaginary part of the corresponding error function integral are calculated using equations (2) and (3).

The real part after the $g_2^{(1)}(x)$ error function transformation is:

$$\begin{aligned}&\frac{1}{\pi}\int_0^{2\pi} g_2^{(1)}(t)\sin t dt\\&=\frac{1}{\pi}\left(-\int_0^{\frac{\pi}{2}}\cos t\sin t dt+\int_{\frac{\pi}{2}}^{\pi}\cos t\sin t dt\right.\\&\quad\left.-\int_{\pi}^{\frac{3\pi}{2}}\cos t\sin t dt+\int_{\frac{3\pi}{2}}^{2\pi}\cos t\sin t dt\right)\\&=-\frac{2}{\pi}\end{aligned}\tag{21}$$

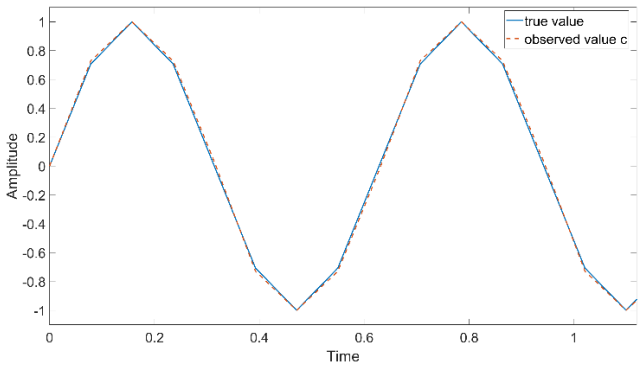

FIGURE 6. Harmonic figure error of case 2 with m = 10.

The imaginary part after the $g_2^{(1)}(x)$ error function transformation is:

$$\begin{aligned}&\frac{1}{\pi}\int_0^{2\pi} g(t)_2^{(1)}\cos t dt\\&=\frac{1}{\pi}\left(-\int_0^{\frac{\pi}{2}}\cos t\cos t dt+\int_{\frac{\pi}{2}}^{\pi}\cos t\cos t dt\right.\\&\quad\left.-\int_{\pi}^{\frac{3\pi}{2}}\cos t\cos t dt+\int_{\frac{3\pi}{2}}^{2\pi}\cos t\cos t dt\right)\\&=0\end{aligned}\tag{22}$$

The real part of the original signal function is:

$$\frac{1}{\pi}\int_0^{2\pi}\sin t\sin t dt=1\tag{23}$$

The imaginary part of the original signal function is:

$$\frac{1}{\pi}\int_0^{2\pi}\sin t\cos t dt=0\tag{24}$$

From the calculation, in this case, the imaginary part of the original signal and the error signal are both 0, one of the real parts is positive, and the other is negative, so they are vectors with completely opposite directions. Then, the maximum relative error of each harmonic is equal to:

$$R_2^{(1)}\max=-2\frac{A0.512}{\pi}\left(\frac{m\pi}{N}\right)^3=-A10.105\left(\frac{m}{N}\right)^3\tag{25}$$

2) CASE 2

Based on the real value, an amount far away from the coordinate axis is added, i.e., error is increased in the direction of the original curve, and a maximum positive error is obtained. The points are as described in the c-curve of the observed value in Figure 6 (Figure 7 is a local enlarged view of Figure 6).

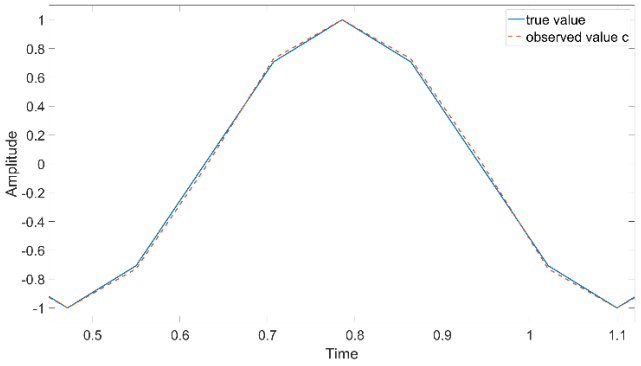

FIGURE 7. Figure error of partial cycle amplification of m = 10 harmonic in case 2.

In this case, error function $R_2^{(2)}$ can be written as:

$$R_2^{(2)}(\mathrm{t}) = \begin{cases} \mathrm{A}0.512\cos(m\omega\mathrm{t})(\frac{m\pi}{N})^3 & 2\mathrm{k}\pi \le m\omega\mathrm{t} \le 2\mathrm{k}\pi + \frac{\pi}{2} \\ -\mathrm{A}0.512\cos(m\omega\mathrm{t})(\frac{m\pi}{N})^3 & 2\mathrm{k}\pi + \frac{\pi}{2} \le m\omega\mathrm{t} \le 2\mathrm{k}\pi + \pi \\ \mathrm{A}0.512\cos(m\omega\mathrm{t})(\frac{m\pi}{N})^3 & 2\mathrm{k}\pi + \pi \le m\omega\mathrm{t} \le 2\mathrm{k}\pi + \frac{3\pi}{2} \\ -\mathrm{A}0.512\cos(m\omega\mathrm{t})(\frac{m\pi}{N})^3 & 2\mathrm{k}\pi + \frac{3\pi}{2} \le m\omega\mathrm{t} \le 2\mathrm{k}\pi + 2\pi \end{cases} \tag{26}$$

In this case, the error calculation is similar to that in the first case, except the error signal and original signal have the same direction, and the relative error of each harmonic is exactly identical.

$$R_2^{(2)}\max = -A10.105\left(\frac{\mathrm{m}}{N}\right)^3 \tag{27}$$

3) CASE 3

The error function is a simple $\cos(\xi)$ function:

$$\begin{aligned} R_2^{(3)}(\mathrm{t}) &= A0.512\cos(\mathrm{t}) \times (\frac{m\times\pi}{N})^3 \\ \mathrm{Or}R_2^{(3)}(\mathrm{t}) &= -\mathrm{A}0.512\cos(\mathrm{t}) \times (\frac{m\times\pi}{N})^3 \end{aligned} \tag{28}$$

At this time, the phase difference $\frac{\pi}{2}$ between the error signal and the original signal function is the maximum calculated phase-angle error. The points are described in the d-curve of the observed values in Figure 8 (Figure 9 is a local enlarged view of Figure 8).

In this case, a vector perpendicular to the original vector is superimposed. In this case, the original vector and error vector can be combined using the parallelogram rule.

After Fourier transformation, the real part is 0, and the imaginary part is $-A0.512(\frac{m\pi}{N})^3$. The calculation results show that the error function and original signal are perpendicular to each other, so the synthesis of the two vectors

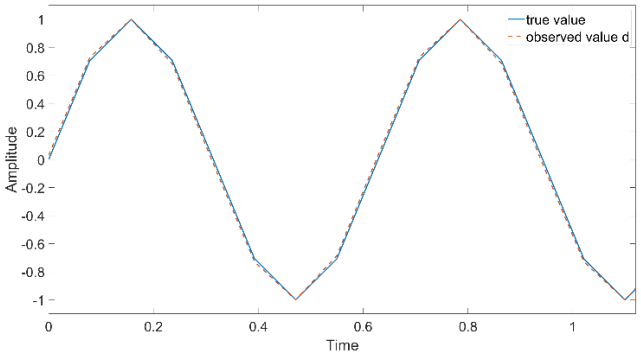

FIGURE 8. Harmonic figure error of case 3 with m = 10.

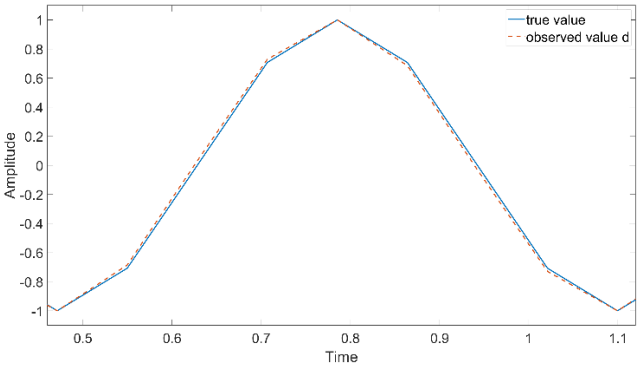

FIGURE 9. Figure error of the partial cycle amplification of m = 10 harmonic in case 3.

TABLE 3. When N = 80, the theoretical error value of each harmonic in the three cases.

Harmonic number	Theoretical error of mode 1	Theoretical error of mode 2	Theoretical error of mode 3
1	-0.00002	0.00002	0
2	-0.0002	0.0002	0.000000003
13	-0.04	0.04	0.001
15	-0.06	0.06	0.005
20	-0.15	0.15	0.003
25	-0.3	0.3	0.11

should follow the parallelogram rule. The modulus of the synthesized vector, i.e., the maximum relative error of each harmonic analysis in the third case, is:

$$R_2^{(3)}\max = \sqrt{1 + [\mathrm{A}0.512(\frac{m\pi}{N})^3]^2} \tag{29}$$

The angle also changes. According to the above calculation, when the original signal amplitude A is 1 and N is 80, the error of different harmonic times is as shown in Table 3.

If the sampling points N is 200 the errors of different harmonic orders is shown in Tables 4.

According to the above calculation, the maximum error occurs in mode 1 and mode 2. The main error is found to be mode 1 in practice. Furthermore, it can be proven that the error calculation method is also applicable to different harmonic orders m and sampling numbers N.

TABLE 4. When N = 200, the theoretical error value of each harmonic in the three cases.

Harmonic number	Theoretical error of mode 1	Theoretical error of mode 2	Theoretical error of mode 3
1	-0.00000126	0.00000126	0
2	-0.00001011	0.00001011	0
10	-0.00126	0.00126	0.000001969
20	-0.0101	0.0101	0.000126
40	-0.081	0.081	0.008032
60	-0.2728	0.2728	0.088

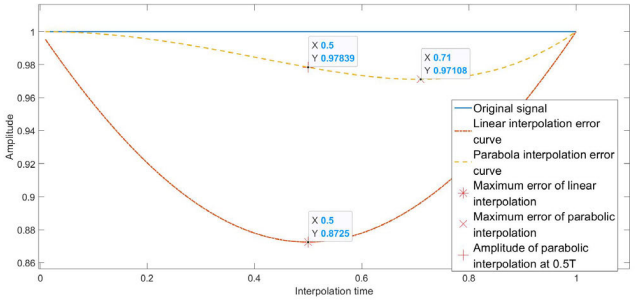

FIGURE 10. Thirteenth harmonic interpolation accuracy.

V. PRACTICAL VERIFICATION

A. SIMULATION

Through MATLAB simulation, interpolation analysis is performed for points at different times within a cycle. After interpolation, the interpolation accuracy of the 13th harmonic is as shown in the figure. The abscissa represents the time (in period) between the position of the interpolation point and the previous data point, and the ordinate is the amplitude signal after Fourier transform in one period (the original signal amplitude is 1):

This simulation experiment aims to study the amplitude changes of the two interpolation methods after calculation within a period T. Figure 10 shows the minimum amplitudes of the two interpolation methods calculated in period T and the amplitudes of the two interpolation methods at 0.5T and 0.7T. When the interpolation time is 0.5T, the minimum amplitude calculated by linear interpolation is 0.8725, and the error is 0.1175. In addition, the amplitude after the parabola interpolation calculation is 0.9784, and the error is 0.0216. When the interpolation time is 0.7T, the minimum amplitude calculated by the parabolic interpolation method is 0.9711, and the error is 0.029.

Similarly, the interpolation accuracy diagrams of the 15th, 20th, and 25th harmonics can be obtained, as shown in Figures 11, 12 and 13.

Figure 13 shows that for the 25th harmonic, the minimum amplitude after linear interpolation at time 0.5T is 0.5556, and the error is 0.4444. At the same time, the amplitude calculated by the parabolic interpolation method is 0.8010, and the error is 0.199. At 0.7T, the calculated amplitude after parabolic interpolation has the smallest amplitude, the smallest amplitude is 0.7226, and the error reaches 0.2774. Therefore,

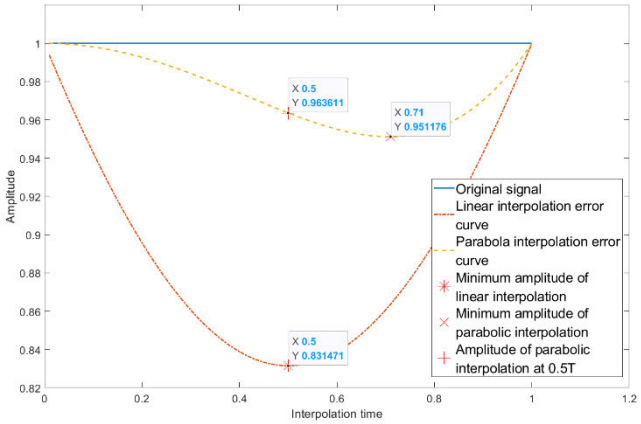

FIGURE 11. Fifteenth harmonic interpolation accuracy (N = 80).

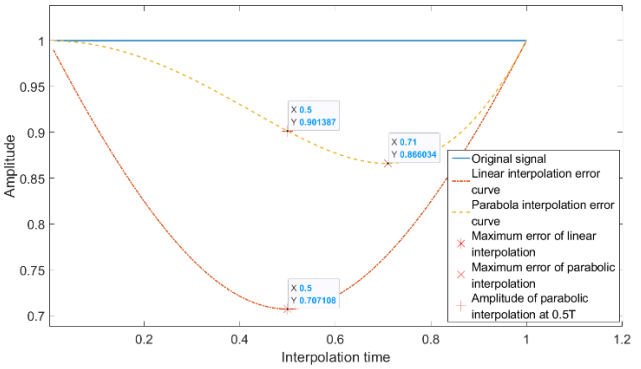

FIGURE 12. Twentieth harmonic interpolation accuracy (N = 80).

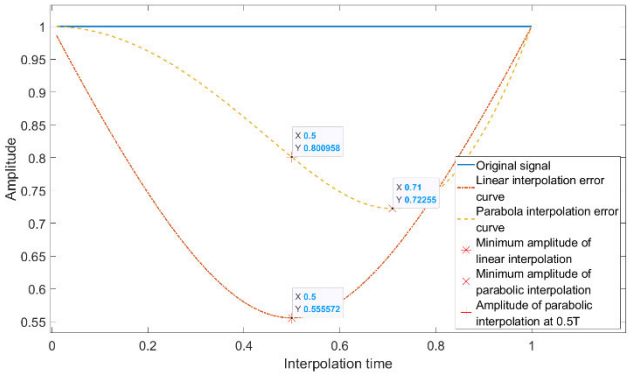

FIGURE 13. Twenty-fifth harmonic interpolation accuracy (N = 80).

whether it is at the same time or simply comparing the minimum error, the parabolic interpolation method has obvious advantages over the linear interpolation method. Based on the same analysis of the 15th and 20th harmonics, conclusions can be drawn.

The minimum amplitude, maximum error and theoretical error of each harmonic in period T under the two interpolation methods are shown in Tables 5 and 6.

Similarly, the interpolation accuracy of 20th and 60th harmonics can be obtained when n = 200, as shown in Figure 14 and Figure 15.

TABLE 5. Analysis of harmonic error of linear interpolation when N = 80.

Harmonic number	Maximum error under linear interpolation theory	Minimum amplitude under linear interpolation	Maximum error under linear interpolation
13	0.13	0.8725	0.1175
15	0.173	0.8315	0.1685
20	0.308	0.7071	0.2929
25	0.48	0.5556	0.4444

TABLE 6. Harmonic error analysis of parabolic interpolation when N = 80.

Harmonic number	Maximum error under parabolic interpolation theory	Minimum amplitude under parabolic interpolation	Maximum error of parabolic interpolation	0.5T parabolic interpolation amplitude	0.5T parabolic interpolation error
13	0.04	0.9711	0.029	0.9784	0.0216
15	0.06	0.9521	0.049	0.9636	0.0364
20	0.15	0.8660	0.134	0.9024	0.0986
25	0.3	0.7226	0.2774	0.8010	0.199

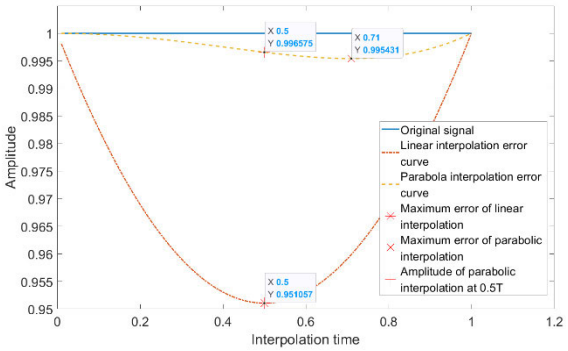

FIGURE 14. Twentieth harmonic interpolation accuracy (N = 200).

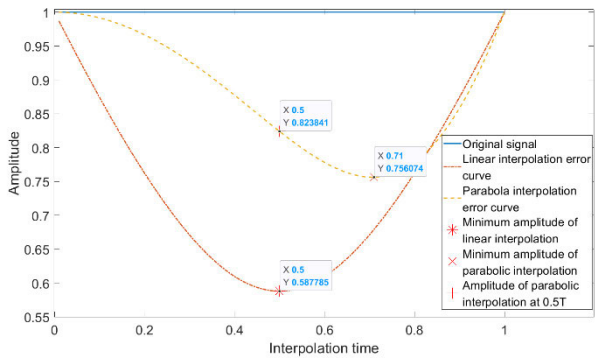

FIGURE 15. Sixtieth harmonic interpolation accuracy (N = 200).

If the sampling points N is 200, the minimum amplitude, maximum error and theoretical error of each harmonic is shown in Tables 7 and 8.

TABLE 7. Harmonic error analysis of linear interpolation when N = 200.

Harmonic number	Maximum error under linear interpolation theory	Minimum amplitude under linear interpolation	Maximum error under linear interpolation
20	0.0493	0.9511	0.0489
60	0.4437	0.5878	0.4122

TABLE 8. Harmonic error analysis of parabolic interpolation when N = 200.

Harmonic number	Maximum error under parabolic interpolation theory	Minimum amplitude under parabolic interpolation	Maximum error of parabolic interpolation	0.5T parabolic interpolation amplitude	0.5T parabolic interpolation error
20	0.0101	0.9954	0.0046	0.9966	0.0034
60	0.2728	0.7561	0.2439	0.8238	0.1762

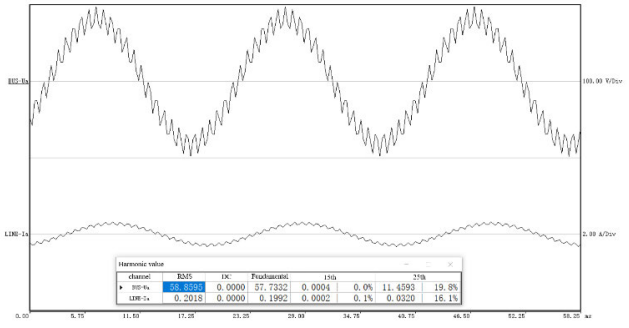

FIGURE 16. 25th harmonic device test waveform.

The charts show that the data of this simulation experiment (N = 80 and 200) is completely consistent with the theoretical calculation data. In the simulation experiment in Tables 5 and Table 7, the harmonic errors of each harmonic of the linear interpolation method are all smaller than the theoretical errors, and there is not much difference. Moreover, the maximum error of the parabolic interpolation method in this simulation experiment in Table 4 and the parabolic interpolation error at 0.5T are both within the theoretical maximum error range. This simulation experiment confirms that the theoretical error calculation of the aforementioned harmonics after the two interpolation methods is correct.

B. DEVICE TEST

The power system fault recorder is a typical recording and measuring device that can record the sampling value of the current and voltage of the power grid in real time when a fault occurs. Therefore, this device is used to verify the scheme of this article. The current and voltage are input from one channel each, and the time difference between the two external samplings is 125 μs.

TABLE 9. Actual error of each harmonic under two interpolation methods.

Harmonic number	Actual error of linear interpolation	Actual error of parabola interpolation	Parabolic interpolation amplitude error at 0.5T under simulation
13	-0.12	-0.02	-0.0216
15	-0.16	-0.03	-0.0364
20	-0.29	-0.09	-0.0986
25	-0.44	-0.19	-0.199

On the basis of simulation analysis, the interpolation characteristics are tested by device. The following 16 shows the test results of the real device.

U_a and I_a are all fundamental waves superimposed with 20% of the 25th harmonic, in which the voltage does not add a delay and does not need interpolation; however, when the current needs to add 125 μs delay, it needs to be interpolated. The result shows that the 25th harmonic of the voltage is still close to 20%, but the 25th harmonic of the current after interpolation is significantly reduced, only 16.1% of the fundamental wave; the error reaches 19.5%.

Based on the same analysis, various interpolation errors of the 13th, 15th, and 20th harmonics at 0.5T are obtained. The data are completely consistent with the simulation analysis data.

Table 9 shows the error of each harmonic manufacturer (the interpolation time is 125 μs) during a wave recorder experiment at Cape Laboratory.

The abovementioned measured data and simulation analysis verified the accuracy of the aforementioned theoretical calculation results.

C. TEST CONCLUSION

Compared with the actual test results and theoretical analysis results, the following conclusions can be drawn:

1) All real test values are within the theoretical calculation range.
2) In the linear interpolation, the actual value is very close to the real value. For example, for the 25th harmonic, the measured error is 44%, and the theoretically calculated value is 48%.
3) For the parabolic interpolation, the actual value is close to the real value. For example, the theoretical value of the 15th harmonic is 6%, and the measured value is 3%, which is a very good result. However, with the increase in harmonic number, there is still a certain gap. For example, for the 25th harmonic, the measured error is 19%, and the theoretically calculated value is 30%; the reason for this difference is that the maximum value calculated in this paper is the worst-case maximum value, but not all points in the actual interpolation encounter this situation.
4) Both interpolation methods can satisfy the requirements for the fundamental and second harmonics. However, parabolic interpolation has much better accuracy than linear interpolation for wave recorders, power quality analyzers and watt hour meters. For example, for the 13th harmonic, the error of linear interpolation is 13% (the actual error is 12%), but the theoretical error of the parabolic interpolation is 4% (the actual error is 2%). Therefore, parabolic interpolation should be selected as much as possible if the conditions permit its selection.

The interpolation accuracy is related to the number of sampling points. According to the above theoretical analysis, when the number of sampling points is doubled, the maximum error of the first-order interpolation is reduced to 1/4 of the previous value, and the maximum error of the second-order interpolation is reduced to 1/8 of the previous value.

VI. CONCLUSION AND RESEARCH PROSPECTS

This paper comprehensively presents maximum theoretical values for the interpolation error when Lagrange linear and second-order approximations of sinusoidal signals are performed and compares it with real test data to verify the correctness.

The maximum theoretical error of linear interpolation is:

$$R_1 \max = A \times 4.93 \times \frac{\mathrm{m}^2}{N^2}$$

The maximum theoretical error of the parabola error is:

$$R_2 \max = A \times 10.105 \times \left(\frac{\mathrm{m}}{N}\right)^3$$

The actual error of the linear interpolation is very close to the theoretical error, and the actual error of the parabolic interpolation is close to the theoretical error.

The focus of this article is to minimize the error value of the harmonics. Traditional research analyzes only the error after interpolation in the form of point-to-point analysis. Furthermore, the conclusion of this paper has a guiding role for intelligent substation harmonic analysis and measurement, which must use the interpolation algorithm.

In addition to the fixed error caused by interpolation, the harmonic error is also closely related to the noise at the time of sampling; therefore, the analysis should be carried out according to the actual situation. According to our conclusion, we can select the appropriate interpolation algorithm and sampling period to improve the harmonic measurement accuracy of the substation.

REFERENCES

[1] J. Li, Y. Cao, X. Zhang, H. Lin, H. Dai, and Y. Xu, "An accurate harmonic parameter estimation method based on Slepian and Nuttall mutual convolution window," *Measurement*, vol. 174, Apr. 2021, Art. no. 109027.

[2] W. Wang, M. Liu, X. Zhao, and G. Yang, "Shared-network scheme of SMV and GOOSE in smart substation," *J. Modern Power Syst. Clean Energy*, vol. 2, no. 4, pp. 438–443, Dec. 2014, doi: 10.1007/s40565-014-0073-z.

[3] D. Li, Z. Zhu, R. Ding, M. Liu, Y. Yang, and N. Sun, "A 10-bit 600-MS/s time-interleaved SAR ADC with interpolation-based timing skew calibration," *IEEE Trans. Circuits Syst. II, Exp. Briefs*, vol. 66, no. 1, pp. 16–20, Jan. 2019, doi: 10.1109/TCSII.2018.2828649.

[4] B. D. Batinic, M. S. Arbanas, J. S. Bajic, S. R. Dedijer, V. M. Rajs, N. M. Lakovic, and N. R. Kulundzic, "Using machine learning for improvement of reflected spectrum estimations of colorimetric probe," *IEEE Trans. Instrum. Meas.*, vol. 70, 2021, Art. no. 2500807, doi: 10.1109/TIM.2020.3011763.
[5] Y. Li, M. Xu, Y. Wei, and W. Huang, "An improvement EMD method based on the optimized rational Hermite interpolation approach and its application to gear fault diagnosis," *Measurement*, vol. 63, pp. 330–345, Mar. 2015.
[6] S. Paquelet, A. Zeineddine, A. Nafkha, P.-Y. Jezequel, and C. Moy, "Convergence of the Newton structure transfer function to the ideal fractional delay filter," *IEEE Signal Process. Lett.*, vol. 26, no. 9, pp. 1354–1358, Sep. 2019, doi: 10.1109/LSP.2019.2929439.
[7] H. Sarbazi-Azad, L. M. Mackenzie, M. Ould-Khaoua, and G. Min, "An efficient parallel algorithm for Lagrange interpolation and its performance," in *Proc. 4th Int. Conf./Exhib. High Perform. Comput. Asia–Pacific Region*, 2000, pp. 593–598, doi: 10.1109/HPC.2000.843503.
[8] W. Luo, J. Liu, Z. Li, and J. Song, "Error analysis of higher order bivariate Lagrange and triangular interpolations in electromagnetics," *IEEE Open J. Antennas Propag.*, vol. 1, pp. 590–597, 2020, doi: 10.1109/OJAP.2020.3030091.
[9] J. Li, Z. Teng, Y. Wang, F. Zhang, and X. Li, "A digital calibration approach for reducing phase shift of electronic power meter measurement," *IEEE Trans. Instrum. Meas.*, vol. 67, no. 7, pp. 1638–1645, Jul. 2018, doi: 10.1109/TIM.2018.2801039.
[10] M. D. Kušljević, "Quasi multiple-resonator-based harmonic analysis," *Measurement*, vol. 94, pp. 471–473, Dec. 2016.
[11] Q. Cai and L. Song, "The Lagrange interpolation polynomial algorithm error analysis," in *Proc. Int. Conf. Comput. Sci. Service Syst. (CSSS)*, Nanjing, China, Jun. 2011, pp. 3719–3722, doi: 10.1109/CSSS.2011.5972217.
[12] B. Zhou, G. Lu, G. Huang, and J. Shen, "A sampled values interface method for substation IED based on the linear Lagrange interpolation algorithm," *Automat. Electr. Power Syst.*, vol. 31, no. 3, pp. 86–90, Feb. 2007.
[13] D. Zhang and L. Jin, "Algorithm for characteristic harmonics analysis based on spectral refinement and interpolation," in *Proc. 2nd IET Renew. Power Gener. Conf. (RPG)*, Beijing, China, 2013, pp. 1–4, doi: 10.1049/cp.2013.1725.
[14] Z. Ye, "Linear phase Lagrange interpolation filter using odd number of basepoints," in *Proc. IEEE Int. Conf. Acoust., Speech, Signal Process.*, Hong Kong, Apr. 2003, p. VI-237, doi: 10.1109/ICASSP.2003.1201662.
[15] V. Valimaki and A. Haghparast, "Fractional delay filter design based on truncated Lagrange interpolation," *IEEE Signal Process. Lett.*, vol. 14, no. 11, pp. 816–819, Nov. 2007, doi: 10.1109/LSP.2007.898856.
[16] A. Candan, "An efficient filtering structure for Lagrange interpolation," *IEEE Signal Process. Lett.*, vol. 14, no. 1, pp. 17–19, Jan. 2007, doi: 10.1109/LSP.2006.881528.
[17] I. Parvez, M. Aghili, A. I. Sarwat, S. Rahman, and F. Alam, "Online power quality disturbance detection by support vector machine in smart meter," *J. Modern Power Syst. Clean Energy*, vol. 7, no. 5, pp. 1328–1339, Sep. 2019, doi: 10.1007/s40565-018-0488-z.
[18] S. Krishnamurthy and B. E. Baningobera, "IEC61850 standard-based harmonic blocking scheme for power transformers," *Protection Control Modern Power Syst.*, vol. 4, no. 1, pp. 121–135, May 2019, doi: 10.1186/s41601-019-0123-7.
[19] W. Zhao, L. Shang, and J. Sun, "Power quality disturbance classification based on time-frequency domain multi-feature and decision tree," *Protection Control Modern Power Syst.*, vol. 4, no. 1, pp. 337–342, Dec. 2019, doi: 10.1186/s41601-019-0139-z.
[20] V. Z. Korac and M. D. Kusljevic, "Cascaded-dispersed-resonator-based Off-nominal-frequency harmonics filtering," *IEEE Trans. Instrum. Meas.*, vol. 70, 2021, Art. no. 1501203, doi: 10.1109/TIM.2020.3035396.
[21] N. Yi-Xiong, P. Xian-gang, D. Qiao-xu, and D. Xiao-kang, "Research on the simple interpolated FFT algorithm for harmonic power energy measurement," in *Proc. 3rd Int. Conf. Instrum., Meas., Comput., Commun. Control*, Shenyang, China, Sep. 2013, pp. 1–5, doi: 10.1109/IMCCC.2013.8.
[22] J. Jiang and S. Qiao, "Essential relation between 1 three-I level SVPWM and SPWM and analysis on output voltage harmonic," *Autom. Electr. Power Syst.*, vol. 39, no. 12, pp. 130–137, Jun. 2015, doi: 10.7500/AEPS20140818009.

ZHAOYUN ZHANG (Senior Member, IEEE) was born in Yichang, China, in December 1977. He received the B.S., M.S., and Ph.D. degrees in electric power engineering from the Huazhong University of Science and Technology, in 2000, 2003, and 2014, respectively. From 2003 to 2016, he was with State Grid Electric Power Research Institute Company Ltd. Since 2016, he has been a Professor with the College of Electronic Engineering and Intelligence, Dongguan University of Technology. His research interests include power systems and protection relay.

QITONG WANG was born in Shanxi, China, in February 1997. He received the B.S. degree in electric power engineering from Tianjin University Renai College, in 2019. He is currently pursuing the M.S. degree with the Guangdong University of Technology.

His main research interests include power systems and protection relay.

ZHI ZHANG received the B.S. degree in automation from Xiangtan University, Xiangtan, China, in 2003, the M.S. degree in power electronics and power drives from Guangxi University, Nanning, China, in 2007, and the Ph.D. degree in power electronics and power drives from the South China University of Technology, Guangzhou, China, in 2010. From 2010 to 2013, he was a Senior Application Engineer with East Group Company Ltd., China. Since May 2013, he has been an Associate Professor with the Department of Electrical Engineering, Dongguan University of Technology, Dongguan, China.